Stress Based Control of a Single-Degree-of-Freedom SMA Actuated Arm

T. Michael Seigler, Mohammad H. Elahinia*, Donald J. Leo, and Daniel J. Inman
Department of Mechanical Engineering
Virginia Polytechnic Institute and State University
Blacksburg, VA 24061
email: tseigler@vt.edu

ABSTRACT

In this paper a nonlinear stress-based controller is designed to position a single-degree-of-freedom shape memory alloy (SMA) actuated manipulator. A three part model was constructed based on the dynamics/kinematics of the arm, the thermomechanical behavior of SMA's, and a heat transfer model consisting of electrical heating and natural convection. A variable structure controller is designed to calculate a desired stress, based on position error. The desired stress is compared with the actual stress which is computed using a Kalman filter. The stress error is then used for control via a proportional-integral (PI) controller. Numerical simulations are performed to investigate tracking performance and robustness. The results demonstrate that the controller design is highly accurate in tracking both stationary and time-varying input signals.

I. INTRODUCTION

The complex nonlinear behavior of shape memory alloys–specifically the co-dependent relationship between stress, martensite fraction, and transformation temperature–presents many challenges with regards to control design for SMA actuated manipulators. Some methods that have been investigated include linear control, pulse width modulation, and nonlinear control [1]–[13]. The shared feature in each of these control designs is that position is used as the feedback state. In this work we present an alternative solution to the control problems of SMA actuators by tracking stress as opposed to position. The benefit of tracking stress in rotating systems is that the nonlinearities due to angular position can, in effect, be cancelled.

Feedback linearization with the addition of a sliding surface (i.e., a variable structure controller) is used to calculate a desired stress in the wire, based on the position error, and is compared with the actual stress that is computed using a Kalman filter. The stress error is then used for feedback control via a proportional-integral (PI) controller.

To investigate stress-based control performance, a three part model was constructed in MATLAB/Simulink based on the dynamics of single-degree-of freedom SMA-actuated arm. The model incorporates the dynamics/kinematics of the arm, the thermomechanical behavior of SMA's, and a heat transfer model consisting of electrical heating and natural convection. Based on the model, numerical simulations are performed to investigate tracking performance and robustness.

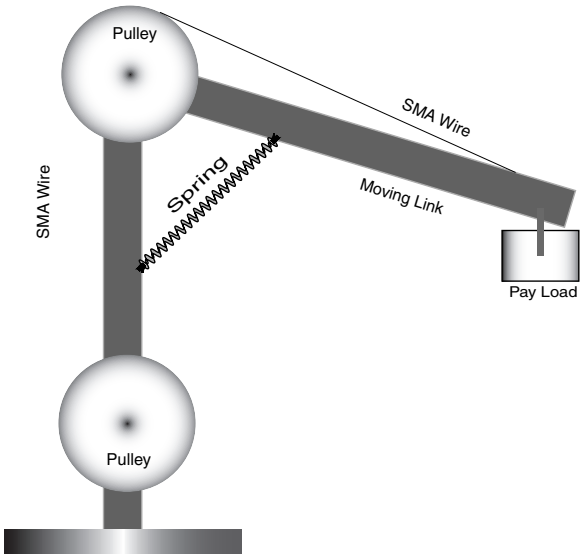

Fig. 1. Diagram of single-degree-of-freedom SMA-actuated arm

II. SMA MANIPULATOR MODEL

The SMA actuated manipulator model consists of three parts: (1)the kinematic/dynamic model, (2) the SMA thermomechanical model, and (3) the heat transfer model. As depicted in Figure 1, the arm is actuated by a bias type actuator constructed with SMA wire, pulleys, and a linear spring. Heating the SMA wire induces a negative strain in the material creating a positive torque and the arm rotates counterclockwise. Conversely, cooling the wire causes the arm to rotate in a clockwise direction. The following sections present the dynamic model used in subsequent numerical simulations. The accuracy of this model has been demonstrated in the experimental work performed by Elahinia and Ashrafiuon [9].

A. Kinematic/Dynamic Model

The dynamic model of the arm including spring and payload effects is represented by

$$I_e\ddot{\theta} + c\ddot{\theta} + [\tau_g(\theta) + \tau_s(\theta)] = \tau_w(\sigma) \tag{1}$$

where $\tau_{\mathrm{w}}, \tau_{\mathrm{g}}$, and τ_{s} are the resulting torques from the SMA wire, gravitational loads, and the bias spring, respectively, and σ is the wire stress. I_e is the effective mass moment of inertia of the arm, gripper, and the payload, and c is the torsional damping coefficient approximating the net joint friction. For simplicity, the above dynamic equation can be expressed as

$$I_e\ddot{\theta} + h(\theta, \dot{\theta}) = \tau_w(\sigma) \tag{2}$$

Report Documentation Page

Form Approved
OMB No. 0704-0188

1. REPORT DATE	2. REPORT TYPE	3. DATES COVERED
00 JUN 2003	**N/A**	**-**

4. TITLE AND SUBTITLE	5a. CONTRACT NUMBER
Stress Based Control of a Single-Degree-of-Freedom SMA Actuated Arm	5b. GRANT NUMBER
	5c. PROGRAM ELEMENT NUMBER
6. AUTHOR(S)	5d. PROJECT NUMBER
	5e. TASK NUMBER
	5f. WORK UNIT NUMBER
7. PERFORMING ORGANIZATION NAME(S) AND ADDRESS(ES) **Department of Mechanical Engineering Virginia Polytechnic Institute and State University Blacksburg, VA 24061**	8. PERFORMING ORGANIZATION REPORT NUMBER
9. SPONSORING/MONITORING AGENCY NAME(S) AND ADDRESS(ES)	10. SPONSOR/MONITOR'S ACRONYM(S)
	11. SPONSOR/MONITOR'S REPORT NUMBER(S)

12. DISTRIBUTION/AVAILABILITY STATEMENT
Approved for public release, distribution unlimited

13. SUPPLEMENTARY NOTES
See also ADM001697, ARO-44924.1-EG-CF, International Conference on Intelligent Materials (5th) (Smart Systems & Nanotechnology)., The original document contains color images.

14. ABSTRACT

15. SUBJECT TERMS

16. SECURITY CLASSIFICATION OF:			17. LIMITATION OF ABSTRACT	18. NUMBER OF PAGES	19a. NAME OF RESPONSIBLE PERSON
a. REPORT	b. ABSTRACT	c. THIS PAGE			
unclassified	**unclassified**	**unclassified**	**UU**	**5**	

where $h(\theta, \dot{\theta})$ now includes viscous damping and the spring and gravitational terms. The SMA wire strain rate $\dot{\varepsilon}$ and joint angular velocity $\dot{\theta}$ are related kinematically as

$$\dot{\varepsilon} = -\frac{2r_{\mathrm{p}}\dot{\theta}}{l_0} \tag{3}$$

where r_{p} is pulleys radius and l_0 is the initial length of SMA wire.

B. Thermomechanical Model

As detailed in the work of Liang and Rogers [14], the thermomechanical behavior of SMAs can be described in terms of strain (ϵ), martensite fraction (ξ), and temperature (T). In the most general form, the mechanical constitutive equation is

$$d\sigma = D(\epsilon, \xi, T)d\epsilon + \Omega(\epsilon, \xi, T)d\xi + \Theta(\epsilon, \xi, T)dT \tag{4}$$

where $D(\epsilon, \xi, T)$ is representative of the modulus of the SMA material, $\Omega(\epsilon, \xi, T)$ is the transformational tensor, and $\Theta(\epsilon, \xi, T)$ is related to the thermal coefficient of expansion.

C. Heat Transfer Model

The assumed SMA wire heat transfer equation consists of electrical heating and natural convection:

$$mc_p\frac{dT}{dt} = \frac{V^2}{R} - hA_c(T - T_\infty) \tag{5}$$

where R is resistance per unit length, c_p is the specific heat, m is mass per unit length and A_c is circumferential area of the SMA wire. Also, V is the applied voltage, T_∞ is the ambient temperature, and h is heat convection coefficient.

III. Control Design

In order to create an improved controller design we first attempt to produce a linear control law based on stress rather than angular displacement. A simple proportional-integral (PI) controller is then used to input a voltage to the wire by tracking the desired stress. It is worth noting that much of the discussion provided here is simplified somewhat for breadth. A more thorough discussion of variable structure control of robotic manipulators can be found in [15]–[18].

Recalling the dynamic equation of motion for the SMA manipulator, Equation 2, we choose the input to be

$$\tau_w(\sigma) = I_e v + h(\theta, \dot{\theta}) \tag{6}$$

which cancels the effects of damping and the torque due to both gravity and the spring. This results in the linear equation

$$\ddot{\theta} = v \tag{7}$$

The task is then to design v in a way that the tracking error converges to zero. Defining the error, e, as the difference between the desired position, θ^d, and the true position, we can define

$$v = \ddot{\theta}^d - k_1\dot{e} - k_0 e + Ksat(s) \tag{8}$$

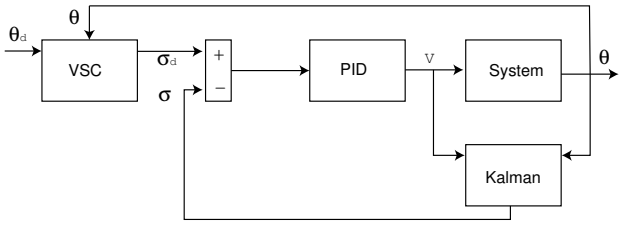

Fig. 2. Block diagram of control design including both feedforward and feedback loops

where k_0 and k_1 are the position and velocity error gains and the saturation term is added to account for model uncertainty. Combining Equations 7 and 8 results in

$$\ddot{e} + k_1\dot{e} + k_0 e = Ksat(s) \tag{9}$$

which, for positive k_0 and k_1, guarantees that the error will converge to zero in finite time [17]. The error dynamics can thus be controlled by a process of selecting the the error gains, k_0 and k_1, and the sliding control gain, K.

Now, given a desired arm angle, the desired torque can be calculated by Equation 6. Note that this desired torque can be converted to a desired stress via the simple kinematic relation

$$\sigma^d = \frac{\tau_w}{Alsin\theta_w} \tag{10}$$

where A is the cross-sectional area of the wire, l is the length of the arm, and θ_w is the constant angle between the SMA wire and the arm. The problem of controlling the SMA arm, however, still remains; that is, how to derive an appropriate voltage given the desired torque. This problem is solved using a proportional-integral (PI) controller. As shown in the block diagram of Figure 2, given the actual and desired stress, the variable structure controller calculates the appropriate stress. It is assumed that the arm angle can be measured with an encoder. The stress in the wire, however, can not be readily measured. To alleviate this problem a Kalman filter is employed to find the stress based on angular position and the voltage input. The design of the Kalman filter is not discussed here, however the reader is directed to [19], [20] for a detailed discussion. Again referring to Figure 2, the predicted stress from the Kalman filter is compared with the desired stress from the variable structure controller and the error is fed through a PI controller that calculates the input voltage by

$$V(t) = K_p(\sigma - \sigma^d) + K_i\int_0^t (\sigma - \sigma^d)\ \ dt \tag{11}$$

where K_p and K_i are the proportional and integral gain, respectively.

IV. Results

The following sections investigate the performance of the controller design presented in the previous section. Numerical simulations, performed in MATLAB/Simulink, are used to implement the two-part controller design with the purpose of evaluating tracking performance and robustness. A linear PID controller, based solely on angular position error, is used for comparison.

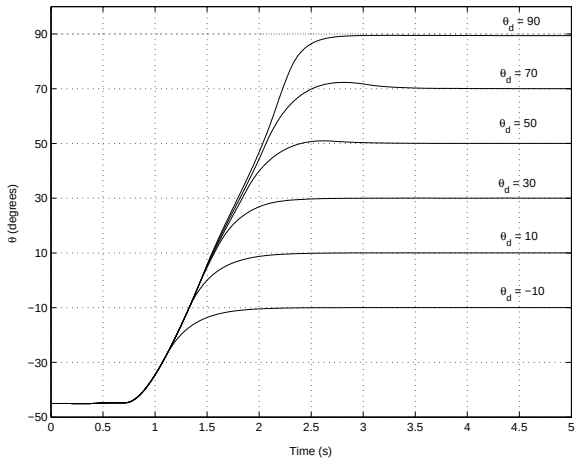

Fig. 3. Controller performance in tracking a desired step

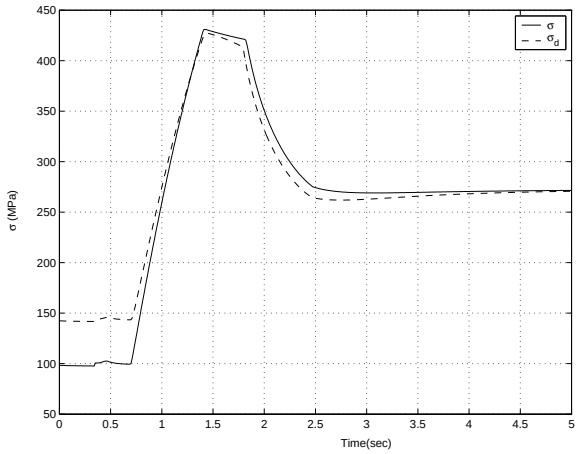

Fig. 4. Tracking desired stress for a 45-degree desired angular position

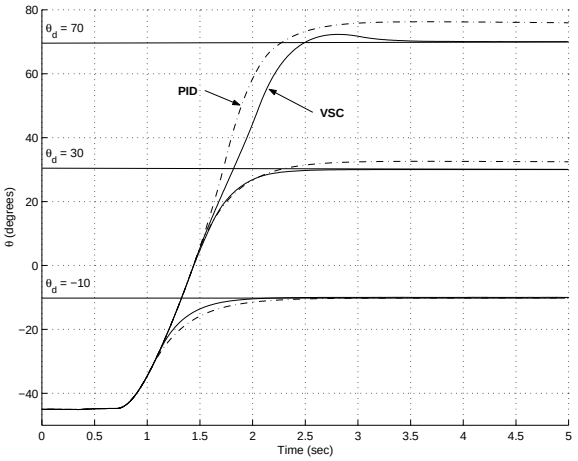

Fig. 5. Control performance comparison of VSC controller and a simple PID controller

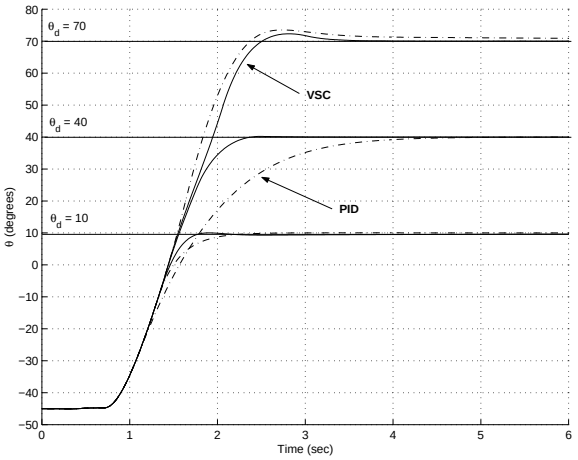

Fig. 6. Control performance comparison of VSC controller and a simple PID controller with optimized gains at each step

A. Control Performance

The control performance in the tracking of a step input can be seen in Figure 3, for a range of inputs from -10 to 90 degrees. Settling times of around 2 seconds are shown for lower angles and around 3.5 seconds for larger angles. Also, some overshoot is evident for angles above 30 degrees. This phenomena is due to the sharp reduction in gravity induced stress as the arm passes the angle of maximum torque as shown in Figure 4.

Figures 5 and 6 show that the variable structure controller (VSC) performs better than a PID controller based solely on the angular position error, $e(t)$. In Figure 5 the PID gains were optimized at 22 degrees–representing half of the arm's range and the angle of maximum stress. It is evident that at angles above 30 degrees, PID control results in large overshoot and settling time. In Figure 6, the PID gains were optimized at each desired arm angle to demonstrate that, even with a variable gain PID controller, the problems with overshoot and settling time remain.

In Figure 7, a desired angular displacement in the form of a 40-degree amplitude, 1 rad/sec sinusoid is input into the controller. After approximately 2 seconds relatively close tracking is achieved. The only significant errors occur at times when the angular velocity exceeds the desired value. It is important to note that the tracking performance of a sinusoidal signal–as well as any time-varying input–is dependent on the input frequency. There are time constants associated with heating and cooling of the wire that prohibit high frequency response.

The final variable input tracking simulation is based on a pseudo-random user input of Figure 8. This input might be typical of that produced by a joystick control. Again, tracking performance is based on physical limitations of the SMA's speed of response, however the desired path is followed with good accuracy.

B. Parameter Uncertainty

The final item of interest is robustness. That is, given some uncertainty due to parameter estimation and model simplification, will the controller continue to perform adequately. In the following simulations, it is assumed that the model is accurately defined, however we include some parameter error in the feedback linearization to examine the effects of uncertainty. Specifically, the mass moment of inertia, I_e, is

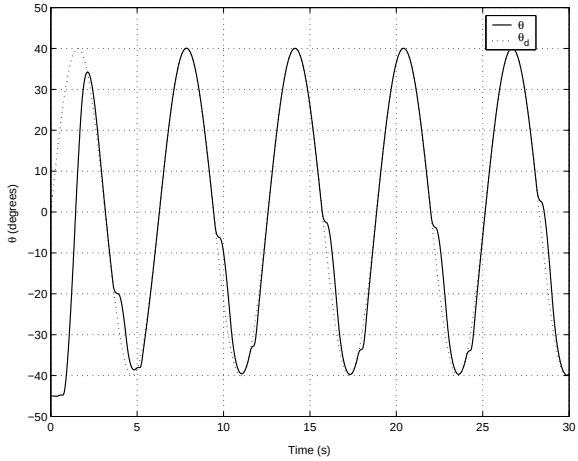

Fig. 7. VSC controller performance in tracking a 40 degree amplitude, 1 rad/sec sinusoidal path

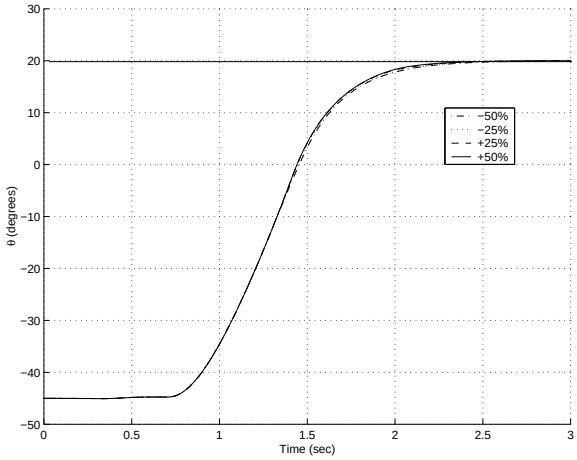

Fig. 9. Effects of estimation errors in the mass moment of inertia, I_e; errors are varied from -50% (underestimation) to +50% (overestimation)

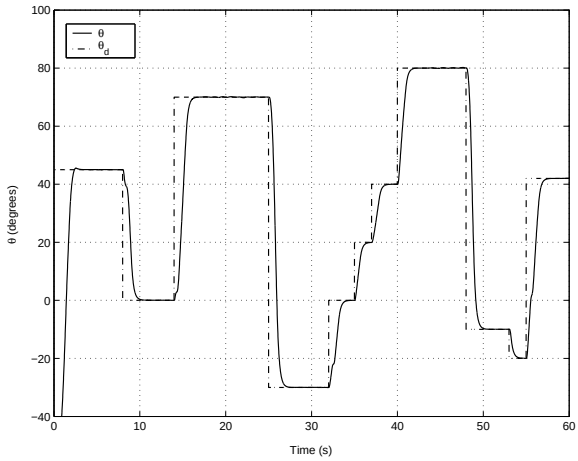

Fig. 8. VSC controller performance in tracking random user commands

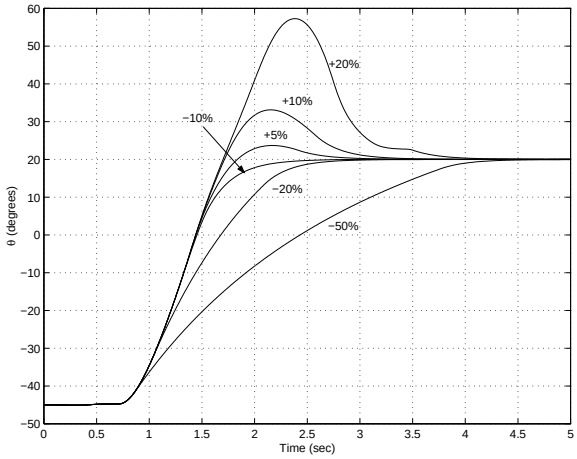

Fig. 10. Effects of estimation errors in damping; errors are varied from -50% (underestimation) to +20% (overestimation)

varied from -50% underestimation to +50% overestimation. Similarly, damping uncertainty is simulated in a range of -50% underestimation to +20% overestimation. The simulations were performed by inputting the false estimations into the VSC controller of Figure 2. In theory, this would produce error in the desired stress calculation resulting in reduced tracking performance.

The results of these simulations are shown in Figures 9 and 10. Referring to Figure 9, the uncertainty in I_e has very little affect on the tracking performance. This is primarily because the inertia term is tied directly to sliding surface component as described by Equation 6. Conversely, as shown in Figure 10, both overestimation and underestimation of the true damping results in either large overshoot or slow settling times. This result is certainly expected, since overestimation in damping would result in a lower desired stress, and underestimation would result in a higher desired stress.

V. Conclusion

A two-stage stress based controller was designed to track desired angular positions of an SMA actuated manipulator. The controller was designed such that, based on position error, a desired wire induced stress is computed by a variable structure controller. The actual stress of the wire, estimated with a Kalman filter, is then used to create a stress error signal. Based on this error signal, a proportional-integral controller is implemented to input a suitable voltage into the wire. The benefit of the additional stress feedback loop is that the nonlinearities in wire stress due to angular position can, in effect, be cancelled. Therefore, the problem is essentially reduced to a hanging mass system.

A model consisting of the dynamic/kinematic relations, the SMA constitutive behavior, and heat transfer within the wire was constructed in MATLAB/Simulink for the purpose of evaluating the controller design. From the numerical simulations, satisfactory results have been shown in terms of tracking both stationary and time-varying input signals. Tracking performance of time-varying inputs, however, is limited to lower frequency signals due to physical limitations of the SMA's speed of response. Furthermore, the stress-based tracking method is shown to demonstrate superior performance over a simple PID controller–based solely on angular position–in terms of rise time, settling time, and overshoot. With

regards to parameter uncertainty, it was shown that large errors in damping estimation can result in undesirable tracking performance.

REFERENCES

[1] S. Arai, K. Aramaki and Y. Yanagisawa. Continuous system modeling of shape memory alloy (SMA) for control analysis. *Proceedings of the 5th IEEE International Symposium on Micro Machine and Human Science*, pages 97–99, 1994.

[2] K. Ikuta. Micro/miniature shape memory alloy actuator. *IEEE Robotics and Automation Society, Los Alamitos, CA. IEEE Computer Society Press*, 3:2156–2161, 1990.

[3] D. Reynaerts and H. Van Brussel. Development of a SMA high performance robotic actuator. *Fifth International Conference on Advanced Robotics, New York*, 2:19–27, 1991.

[4] M. A. Gharaybeh and G. C. Burdea. Investigation of a shape memory alloy actuator force-feedback masters. *Advanced Robotics*, 9(3):317–329, 1995.

[5] M. Hashimoto, M. Takeda, H. Sagawa, and I. Chiba. Application of shape memory alloy to robotic actuators. *Journal of robotic systems*, 2(1):3–25, 1985.

[6] K. Kuribayashi. A new actuator of a joint mechanism using NiTi alloy wire. *The International Journal of Robotics Research*, 4(4):103–108, 1986.

[7] S. Arai, K. Aramaki and Y. Yanagisawa. Feedback linearization of SMA(Shape Memory Alloy). *Proceedings of the 34th SICE Annual Conference*, pages 519–522, 1995.

[8] S. Choi and C. C. Cheong. Vibration control of flexible beam using shape memory alloy actuators. *Journal of Guidance Control, and Dynamics*, 19(5):1178–1180, 1996.

[9] M. H. Elahinia and H. Ashrafiuon. Nonlinear control of a shape memory alloy actuated manipulator. *ASME Journal of Vibration and Acoustics*, 124:566–575, October 2002.

[10] D. Grant and V. Hayward. Vibration isolation with high strain shape memory alloy actuators: case of the impulse disturbance. *In Proceedings of International Mechanical Engineering Congress and Exposition*, 229, 1998.

[11] D. Grant and V. Hayward. Constrained force control of shape memory alloy actuators. *Proceedings of the IEEE International Conference on Robotics and Automation*, pages 1314–1320, 2000.

[12] P. Kumagai, A. Hozian and M Kirkland. Neuro-fuzzy model based feedback controller for Shape Memory Alloy actuators. *Proceedings of SPIE - The International Society for Optical Engineering, Society of Photo-Optical Instrumentation Engineers, Bellingham, WA, USA*, 3984:291–299, 2000.

[13] V. Song, G. Chaudhry and B. Batur. Precision tracking control of shape memory alloy actuators using nueral networks and sliding-mode based robust controller. *Smart Materials and Structures*, 12:223–231, 2003.

[14] C. Liang and C. A. Rogers. One-dimensional thermomechanical constitutive relations for shape memory materials. *Journal of Intelligent Material Systems and Structures*, 1(2):207–234, 1990.

[15] J.J. Slotine. Robust control of robot manipulators. *International Journal of Robotic Research*, 4(2), 1985.

[16] J.J. Slotine and S.S. Sastry. Tracking control of nonlinear systems using sliding surfaces with application to robot manipulators. *International Journal of Control*, 38:465–492, 1983.

[17] M. W. Spong and M. Vidyasagar. *Robot Dynamics and Control*. John Wiley & Sons, 1989.

[18] M.W. Spong and M. Vidyasagar. Robust linear compensator design for nonlinear robotic control. *IEEE Journal of Robotics and Automation*, RA-3(4):345–351, 1987.

[19] Ashrafiuon H. Ahmadian A. Elahinia, M. H. and W. T. Baumann. Design of extended kalman filter for a shape memory alloy manipulator. *Proceedings of the ASME Design Engineering Technical Conferences, September 2-6, 2003, Chicago, Illinois*, September 2003.

[20] Ashrafiuon H. Ahmadian A. Elahinia, M. H. and Inman D. J. Application of the extended kalman filter to control of a shape memory alloy arm. *Proceedings of the ASME Design Engineering Technical Conferences, September 2-6, 2003, Chicago, Illinois*, September 2003.